DYNAMICS, INC.

TR-3-513

ENVIRONMENTAL ATTENUATION OF AIRBORNE RADAR

8 March 1982

BOK
DYNAMICS, INC.

TR-3-513

ENVIRONMENTAL ATTENUATION

OF AIRBORNE RADAR

8 March 1982

Authors: Bruce J. Spaulding
George N. Baum
Ira F. Kuhn, Jr.

B-K Dynamics, Inc.
3204 Monroe Street
Rockville, MD 20850

Sponsored by

Defense Advanced Research Projects Agency (DoD)
ARPA Order No. 4267

Under Contract No. MDA-903-81-C-0313 issued by
Department of Army, Defense Supply Service-Washington,
Washington, DC 20310

UNCLASSIFIED

SECURITY CLASSIFICATION OF THIS PAGE (When Data Entered)

REPORT DOCUMENTATION PAGE

READ INSTRUCTIONS BEFORE COMPLETING FORM

1. REPORT NUMBER: TR-3-513	2. GOVT ACCESSION NO.: N/A
3. RECIPIENT'S CATALOG NUMBER: A119883	
4. TITLE (and Subtitle): Environmental Attenuation of Airborne Radar	5. TYPE OF REPORT & PERIOD COVERED: Technical Report
	6. PERFORMING ORG. REPORT NUMBER:
7. AUTHOR(s): Bruce J. Spaulding, Ira F. Kuhn, Jr., George N. Baum	8. CONTRACT OR GRANT NUMBER(s): MDA-903-81-C-0313
9. PERFORMING ORGANIZATION NAME AND ADDRESS: B-K Dynamics, Inc., Box 6012, 3204 Monroe Street, Rockville, Maryland 20850	10. PROGRAM ELEMENT, PROJECT, TASK AREA & WORK UNIT NUMBERS:
11. CONTROLLING OFFICE NAME AND ADDRESS: Defense Advanced Research Projects Agency, 1400 Wilson Boulevard, Arlington, VA, Attn: Program Management/MIS	12. REPORT DATE: 8 March 1982
	13. NUMBER OF PAGES:
14. MONITORING AGENCY NAME & ADDRESS(if different from Controlling Office): Same as Controlling Office	15. SECURITY CLASS. (of this report): Unclassified
	15a. DECLASSIFICATION/DOWNGRADING SCHEDULE: N/A

16. DISTRIBUTION STATEMENT (of this Report)

Unlimited

17. DISTRIBUTION STATEMENT (of the abstract entered in Block 20, if different from Report)

Same as Report

18. SUPPLEMENTARY NOTES

19. KEY WORDS (Continue on reverse side if necessary and identify by block number)

Rain Attenuation
Cloud Attenuation

20. ABSTRACT (Continue on reverse side if necessary and identify by block number)

DD FORM 1 JAN 73 1473 EDITION OF 1 NOV 65 IS OBSOLETE
S/N 0102-014-6601

UNCLASSIFIED

SECURITY CLASSIFICATION OF THIS PAGE (When Data Entered)

SUMMARY

The most stressing weather scenario for a long range airborne radar is looking to the limb of the earth, and beyond, in an extensive precipitating stratiform system. This is due to both the long horizontal path lengths which must traverse the longest dimensions of stratiform clouds and the shortest dimensions of the less frequently occurring thunderstorms. Realistic vertical profiles of cloud density, effective rainfall rate, and temperature were developed for a typical extensive system. Cloud and rainfall attenuations were then calculated for each 1000 foot layer of the system for each of two seasons (fall-spring and winter) over the microwave radar frequencies (L-Band through X-Band). Total two-way path attenuations were then determined for each of three ranges to 200 feet from a 65,000 foot platform: 300 nm, 250 nm, and 200 nm. The total two-way results are given below. Also examined are frequently used values of cloud density and discrepancies between theoretical and empirical values for rainfall attenuation coefficients.

Excess Two-Way Path Loss due to Weather Attenuation (in dB)

	Fall-Spring			Winter		
	200 nm	250 nm	300 nm	200 nm	250 nm	300 nm
L-Band	.25	.36	.51	.21	.31	.41
S-Band	.75	1.08	1.38	.58	.85	1.16
C-Band	2.95	4.34	5.64	2.14	3.16	4.32
X-Band	12.03	17.92	23.91	7.65	11.44	16.19

PREFACE

For several DARPA systems which make use of airborne radar, the relative merit of utilizing various frequency bands for the radar must be considered in assessing future systems capabilities. Operating at higher frequencies yields improved accuracy, resolution, and countermeasure resistance, however results in a heavier system which is subject to greater environmental attenuation. This study was undertaken to assess environmental attenuation aspects of the frequency choice decision process, by quantifying the total impact of atmospheric, cloud, and rain attenuation.

For this analysis, scenarios of worst-case, yet regularly occurring, rainfall conditions were assumed. A large amount of theoretical and experimental data was investigated and correlated. From this information, an atmosphere/cloud/rain attenuation model was developed and calculations were carried out to determine the attenuation of potential search radars at frequencies between L- and X-band.

TABLE OF CONTENTS

ENVIRONMENTAL ATTENUATION OF AIRBORNE RADAR

A. Introduction

Environmental attenuation of microwave radiation is caused by air, clouds, fog, rain, snow, ice, dust, and smoke. Of these, the effects of atmospheric gases and vapors are the best understood and the easiest to estimate, and the effects of water aerosols are the most difficult to measure or predict. The water aerosols causing greatest attenuation are clouds and rain.

For an airborne search radar in the microwave region (L - X-bands), the cloud/rain system with the greatest long range attenuation impact is the extensive precipitating stratus system, primarily consisting of nimbostratus clouds and light rain as shown in Figure 1. Precipitating clouds have much more attenuation than non-precipitating clouds because the typical cloud aerosol drops (and hence total water content) are much larger in the precipitating clouds (perhaps five times as large). In addition to this, there are the losses directly due to the precipitation.

Non-extensive systems, even if heavily precipitating locally as in thunderstorms, may have large attenuations per unit path length but comparatively less total attenuation due to the short total path lengths through the cloud. (For example, the rain attenuation at X-band through the center of a thunderstorm can be as high as 2 dB/km; however, the storm area would be only 2-3 km wide and its location would be rapidly changing.) Thunderstorms, in addition to being non-extensive, are of infrequent occurrence over most of the world, as will be discussed later in Section E. In addition, the individual storm cells are small enough that high speed aircraft cannot remain within or behind a cell for very long.

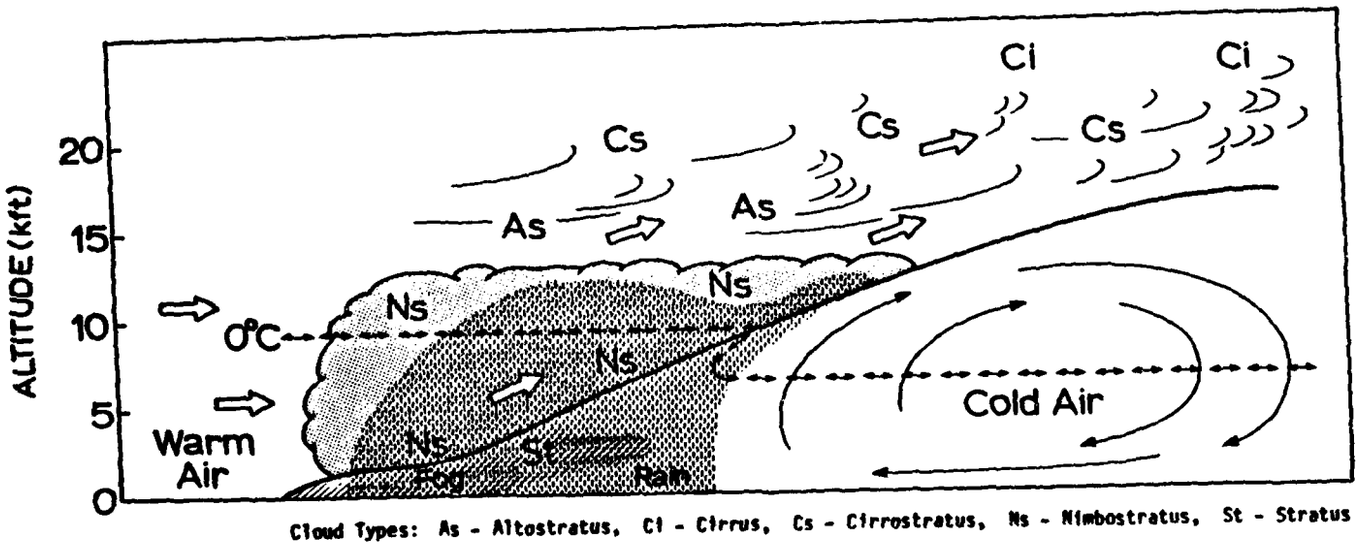

Figure 1. Typical weather conditions and flow patterns observed with warm fronts.

B. Cloud Attenuation

Attenuation by clouds is one of the more stressing effects of weather upon the propagation of microwave radiation. However, the commonly made assumption of a cloud with uniform aerosol density and temperature throughout can substantially overstate the attenuation, particularly in the case of a long range radar looking down through the clouds to the horizon.

In order to determine with increased precision the effects of clouds upon propagation, realistic cloud density and temperature profiles have been used, and the resulting attenuation has been calculated as a function of altitude, over 1,000 ft. altitude intervals. The refracted path of radiation over a curved earth has been determined for several target ranges. The incremental attenuations in each 1,000 ft. layer are then added together and the sum doubled to yield a final figure for two-way transmission through the cloud.

1. Cloud Density Profiles

Typical winter and fall-spring density profiles of nimbostratus clouds, after Prupacher and Klett,[1] are given in Figure 2, for peak water densities of 0.5 gm/m^3, which is representative of winter conditions, and 0.6 gm/m^3, which is representative of fall-spring conditions. This figure is used here as the model for the highest densities of clouds encountered during widespread uniform precipitation. The seasonal conditions are as characterized in the Handbook of Geophysics and Space Environments.[2] Figure 2A (winter) is more sharply skewed with the peak concentrations higher in the cloud compared to Figure 2B (fall-spring), which contains a higher peak concentration and more overall water. Both profiles are typical, however, in that the density increases from a minimum at the base of the cloud to a maximum in the upper

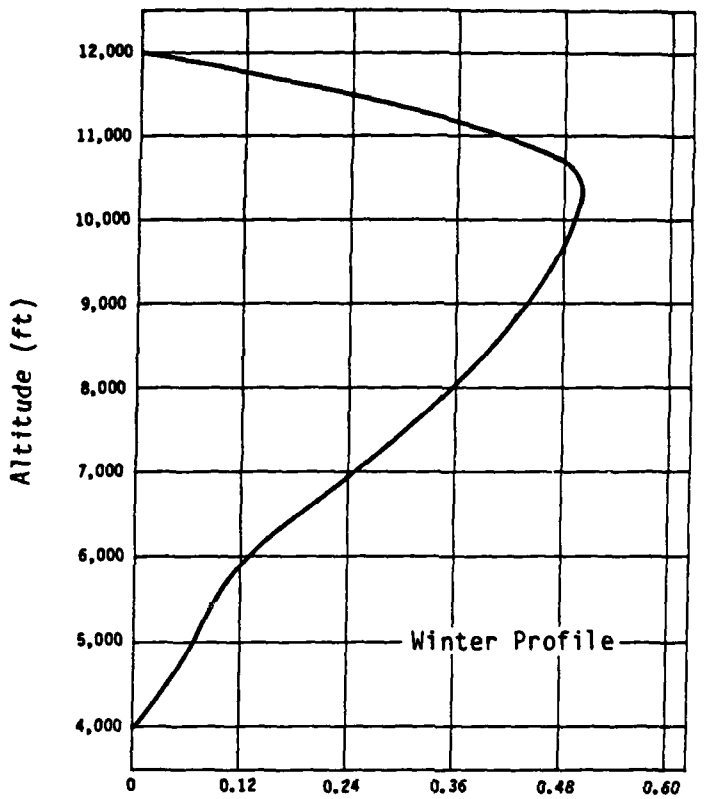

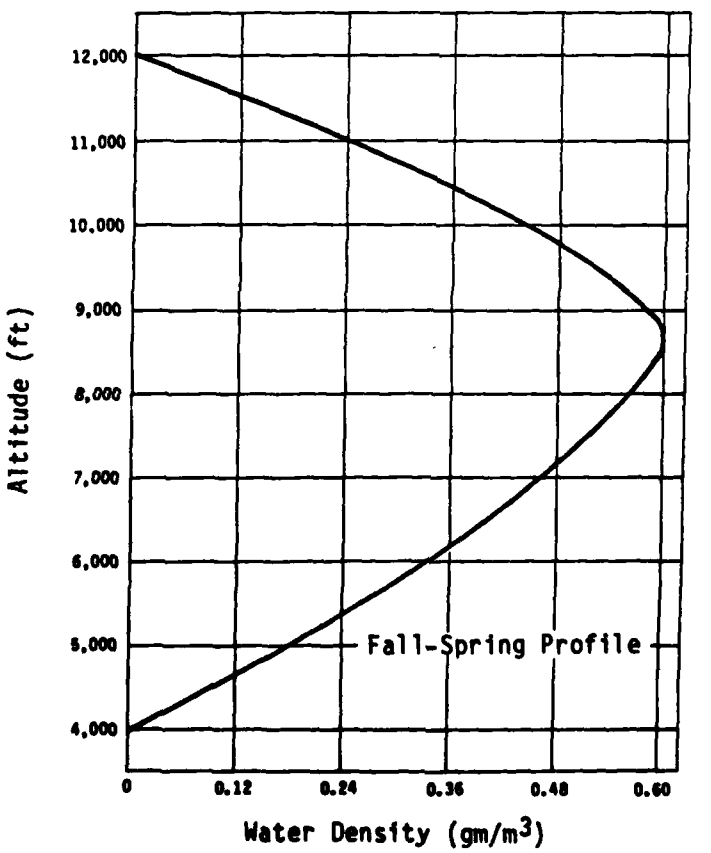

Figure 2. Cloud Water Density Profiles

half of the cloud and then decreases again to a minimum at the cloud's top. The base of the cloud was assumed to be at 4000 feet and its summit at 12,000, this geometry being typical of thick nimbostratus.

The winter profile of Figure 2 has an average density of 0.26 gm/m^3, while the fall-spring profile has an average density of 0.38 gm/m^3. It should be noted that winter clouds tend to have lower densities as the colder air can support less moisture. Other publications (James,[3] Atlas,[4] Mason,[5] Gossard,[6] and Davidson[7]) estimate similar values of average densities, with a mean value being about 0.3 gm/m^3. The use of the higher values of density during the fall-spring season is conservative.

It should be noted at this point that some references have quoted higher cloud density values. For example, Bean et al[8] in the Radar Handbook (referencing Donaldson[9]) state that "the liquid-water concentration in clouds generally ranges from 1 to 2.5 gm/m^3." Bean et al further report the occurrence of "isolated instances of cumulus congestus clouds with a reading of 4.0 gm/m^3 in the upper levels." (Cumulus congestus are similar to the large cumulonimbus thunderstorm clouds.) It appears from these data that the 1-2.5 gm/m^3 refers to dense cumulus-type clouds, which, by nature, are not extensive in breadth, and therefore would yield a lower total attenuation over a long path length than would the more extensive, but lower density nimbostratus cloud frontal system. The matter of cloud densities is discussed in more detail in Appendix A.

2. Cloud Temperature Profiles

Temperature profiles within clouds tend to vary quite extensively even within a given weather system, so mean temperature profiles (horizontally averaged) were used. Since maritime precipitating clouds tend to be about 8°C warmer than continental precipitating clouds at 60°N latitude (see Mason[10]), a value of eight degrees was added to each of the two continental profiles used: fall-spring and winter. The continental profiles used were after Atlas.[2]

TABLE 1
Temperature Profiles

h (ft)	T (°C) Fall-Spring	T (°C) Winter
500	16	7
1,500	14	2
2,500	12	1
3,500	10	2
4,500	8	3
5,500	6	4
6,500	4	2
7,500	2	-1
8,500	0	-5
9,500	-2	-9
10,500	-3	-15
11,500	-5	-20

3. Radar Path Length

Figure 3 shows the basic geometry of surveillance from a high altitude vehicle looking through weather to the limb of the earth. Clouds were assumed to extend from 12,000 down to 4,000 feet and the rain from the 0°C level down to the surface. The path from the target to the radar passes through 57 nm of clouds and an additional 103 nm of rain in the Fall-Spring model or 89 nm of rain in the Winter model. The rain path length difference is due to the differing heights of the freezing layer with the seasons, and therefore the rain altitude.

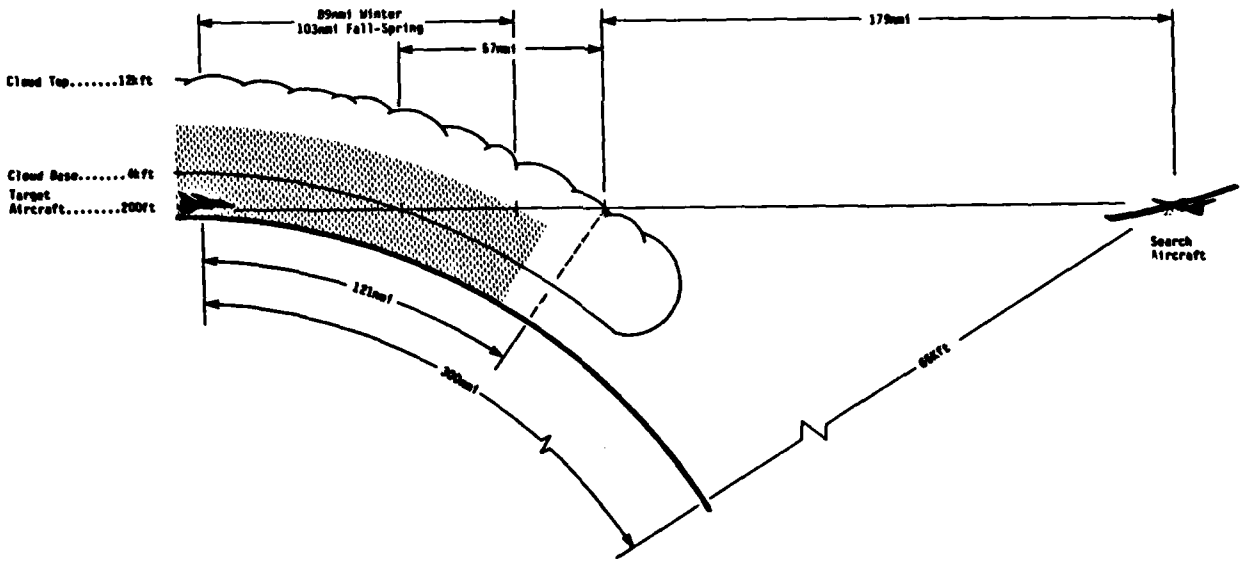

Figure 3. Geometry of Typical Rain and Cloud Scenario

Since both temperature and density vary vertically through the cloud, the cloud was broken into a series of horizontal layers. Because the profiles change slowly with altitude, 1000 foot layers are acceptable. The radar path length within each layer is calculated, assuming the 4/3 earth refraction model. Table 2 gives the path length within each 1000 foot layer.

TABLE 2
Radar Path Lengths

h_L (ft)	h_u (ft)	Δ (nm)
200	1,000	24.38
1,000	2,000	16.67
2,000	3,000	12.63
3,000	4,000	10.52
4,000	5,000	9.24
5,000	6,000	8.12
6,000	7,000	7.66
7,000	8,000	7.16
8,000	9,000	6.68
9,000	10,000	6.36
10,000	11,000	6.01
11,000	12,000	5.77

4. Attenuation Calculation

There are two widely used and essentially similar sources for cloud attenuation data: Ryde and Ryde[11] and Gunn and East.[12] Chen[13] and Goldstein[14] (in Kerr Propagation of Short Radio Waves) both follow Ryde and Ryde. Bean et al[8] (authors of Chapter 24 of Radar Handbook, Skolnik, 1970) follow Gunn and East. At 20°C for X-band, Ryde and Ryde predict a normalized attenuation coefficient of 0.0475 dB/km per gm/m^3 while Gunn and East predict a value of 0.0483 dB/km per gm/m^3, a difference of less than 2%.

The method of Chen[13] is used here for the attenuation calculation:

$$A_C = 0.811 \left\{ \frac{M(h)}{\lambda^2} \right\} \times \Phi(T) \times \Delta \qquad \text{in units of dB,}$$

where: $M(h)$ = cloud water density in gm/m^3

λ = radar wavelength in cm

$\Phi(T)$ = temperature correction factor (dimensionless)

Δ = path length in layer in nm.

The temperature correction factor arises because the index of refraction of water is temperature dependent. The correction factor $\Phi(T)$ is defined:

$$\Phi(T) = \gamma(T)/\gamma(18°C)$$

where γ is attenuation coefficient in dB/nm. Values of $\Phi(T)$ are given in Table 3 after Goldstein:[14]

TABLE 3

Correction Factor $\Phi(T)$

λ, cm	$\Phi(T)$					
	0°C	10°C	18°C	20°C	30°C	40°C
0.5	1.59	1.20	1.0	0.95	0.73	0.59
1.25	1.93	1.29	1.0	0.95	0.73	0.57
3.2	1.98	1.30	1.0	0.95	0.70	0.56
10	2.0	1.25	1.0	0.95	0.63	0.59

Cloud attenuation was then calculated for frequencies of L- through X-bands, using the terms:

$$\gamma(h) = 0.811 \times M(h)/\lambda^2 \qquad \text{dB/nm}$$

$$\gamma(h,T) = \gamma(h) \times \Phi(T) \qquad \text{dB/nm}$$

$$A_C = \gamma(h,T) \times \Delta \qquad \text{dB}$$

An example of these calculations, for the X-band case in a fall-spring cloud, is shown in Table 4:

TABLE 4

X-Band (3.0 cm) Cloud Attenuation for Fall-Spring Maritime Model

h(ft)	T (°C)	M(h) gm/m^3	γ(h) dB/nm	Φ(T)	γ(h,T) dB/nm	Δ nm	A_c dB
4,000							
	8	.12	.0108	1.39	.0150	9.24	.1387
5,000							
	6	.28	.0251	1.50	.0377	8.12	.3062
6,000							
	4	.41	.0373	1.65	.0616	7.66	.4717
7,000							
	2	.53	.0476	1.80	.0856	7.16	.6132
8,000							
	0	.60	.0541	2.00	.1081	6.68	.7222
9,000							
	-2	.55	.0492	2.20	.1082	6.36	.6884
10,000							
	-3	.39	.0352	2.30	.0809	6.01	.4860
11,000							
	-5	.13	.0122	2.50	.0305	5.77	.1757
12,000							3.6022
							2-way 7.20 dB

Table 5 gives the results of the above calculations for L- to X-band in fall-spring and winter temperature and density profiles.

TABLE 5

Cloud Attenuations for L- to X-Band

Radar Band - Wavelength / Model	Fall-Spring Maritime	Winter Maritime
L - 16 cm	0.29 dB	0.24 dB
S - 10 cm	0.64	0.61
C - 5.4 cm	2.26	2.13
X - 3.0 cm	7.20	6.76

5. Detection at Reduced Ranges

The scenario examined above represents maximum range detection by a 65 kft altitude aircraft against a 200 ft altitude target (300 nm), just above the limb of the earth. While this represents the earth-curvature-limited detection range from a high altitude radar, a substantial operational capability is still retained if detection range is reduced to 200 nm by attenuation. For six aircraft at 65,000 feet equally spaced at 300 nm out from the Task Force, a 200 nm radar range would give a range in the notch between radars of nearly 400 nm from the Task Force, as illustrated in Figure 4. Therefore, the weather effects at ranges of 200 and 250 nm were examined.

Figure 5 shows the radar path lengths through clouds and rain for target ranges of 300, 250, and 200 nm. Note that the ranges in clouds and in rain change at different rates, with the biggest change occurring between 300 and 250 nm for clouds as opposed to between 250 and 200 nm for rain.

The first step in examining reduced ranges is to determine the new path lengths in each layer which was done geometrically using the four-thirds earth model for refraction. Table 6 gives the incremental path lengths for the 200 and 250 nm paths.

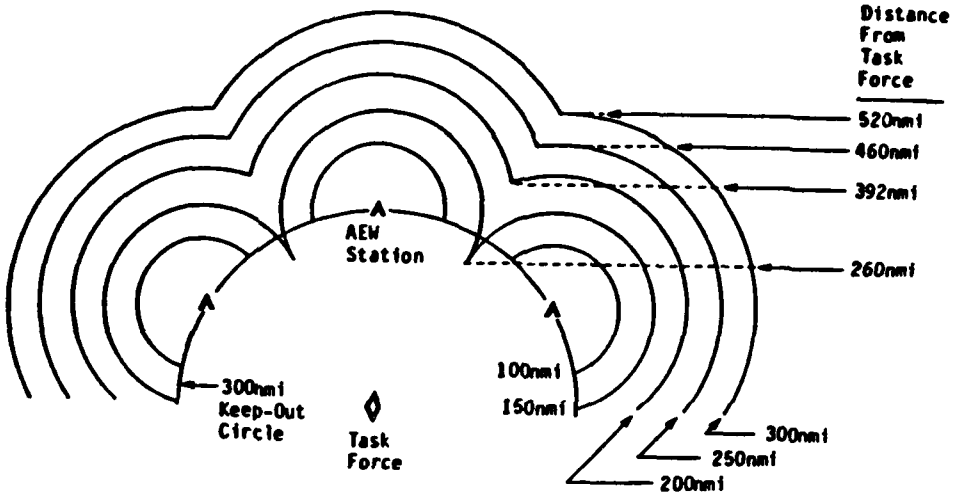

Figure 4. Coverage Patterns for Various Radar Ranges

Radar Range (nmi)	Minimum Coverage Range (nmi)
325	548
300	520
275	491
250	460
225	427
200	392
175	350
150	260

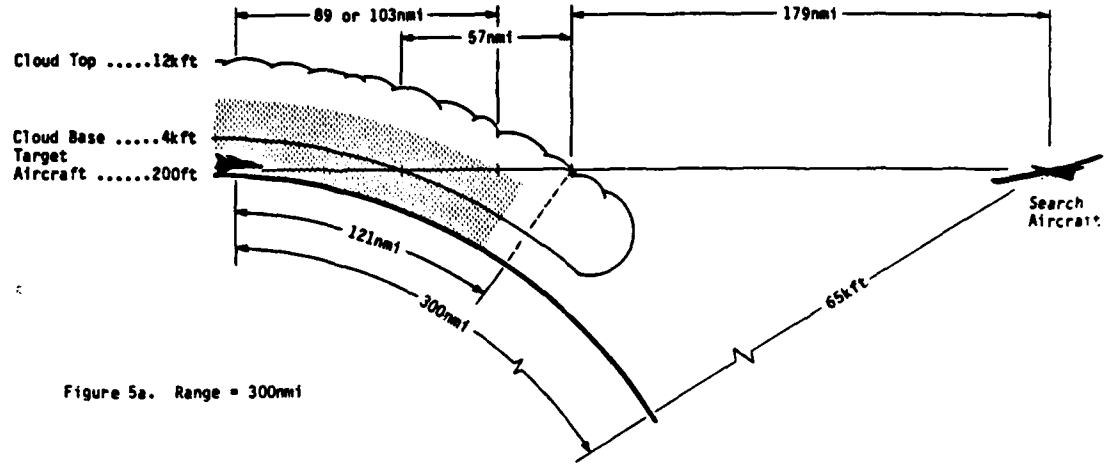

Figure 5a. Range = 300nmi

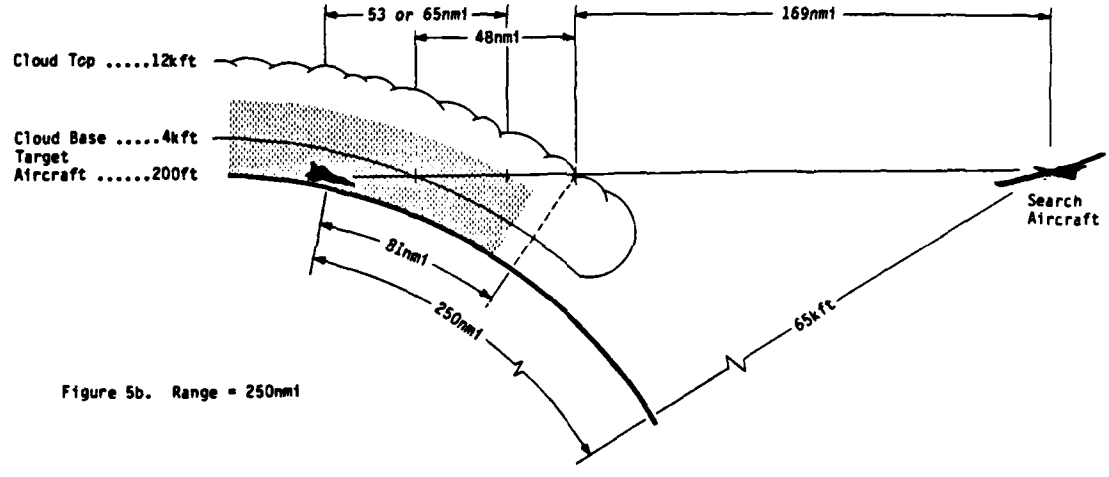

Figure 5b. Range = 250nmi

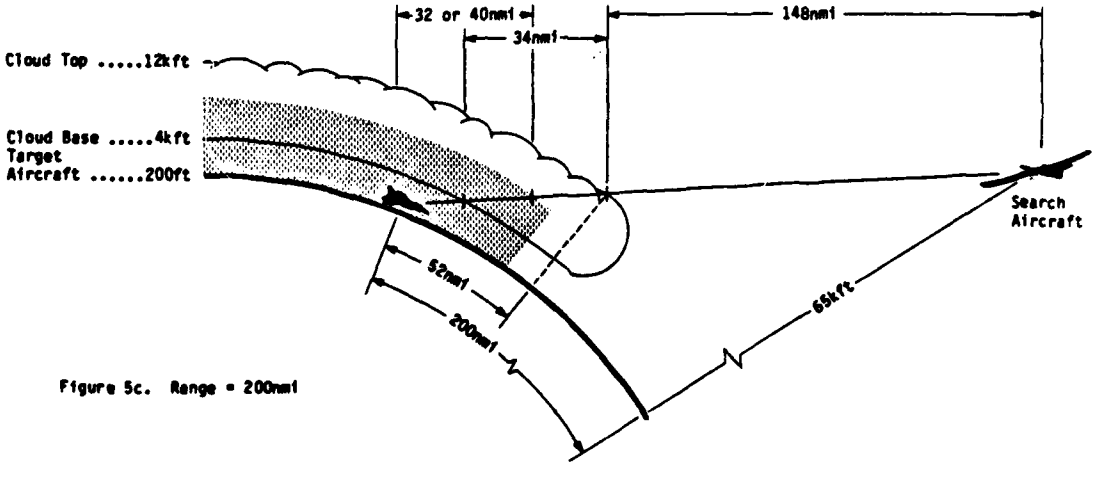

Figure 5c. Range = 200nmi

Figure 5. Radar Paths at Reduced Ranges

TABLE 6

Incremental Path Lengths Through Clouds and Rain from 65 kft to 200 ft Altitude for 250 and 200 nm Ranges

h (ft)	Δ for 250 nm range	Δ for 200 nm range
200		
	8.16 nm	4.15 nm
1,000		
	9.08	5.00
2,000		
	8.27	4.87
3,000		
	7.57	4.70
4,000		
	7.05	4.56
5,000		
	6.66	4.47
6,000		
	6.27	4.31
7,000		
	6.00	4.25
8,000		
	5.70	4.13
9,000		
	5.50	4.06
10,000		
	5.26	3.95
11,000		
	5.11	3.90
12,000		

Once the incremental path lengths are determined, it becomes merely a matter of multiplying these new path lengths by the attenuation factors, $\gamma(h,T)$, already determined for each level. As an example of the process, Table 7 shows the calculations for X-band in the fall-spring cloud.

TABLE 7

X-Band Cloud Attenuation at Reduced Ranges -
Fall-Spring Maritime Model

h feet	200 nm			250 nm		
	$\gamma(h,T)$ dB/nm	Δ nm	A_{cloud} dB	$\gamma(h,T)$ dB/nm	Δ nm	A_{cloud} dB
4,000	.0150	4.56	.0684	.0150	7.05	.1058
5,000	.0377	4.47	.1685	.0377	6.66	.2511
6,000	.0616	4.31	.2655	.0616	6.27	.3862
7,000	.0856	4.25	.3638	.0856	6.00	.5136
8,000	.1081	4.13	.4465	.1081	5.70	.6162
9,000	.1082	4.06	.4393	.1082	5.50	.5951
10,000	.0809	3.95	.3196	.0809	5.26	.4255
11,000	.0305	3.90	.1190	.0305	5.11	.1559
12,000			2.1905			3.0494
		2-way - 4.38 dB			2-Way - 6.10 dB	

Cloud Attenuation at Ranges of 200 nm to 300 nm

The cloud attenuation results for L-band through X-band were calculated for the winter and fall-spring maritime clouds. The results are shown in Table 8.

TABLE 8

2-Way Cloud Attenuations in dB for Various Ranges Given

Winter Maritime

	300 nm	250 nm	200 nm
L-Band	0.24	0.21	0.15
S-Band	0.61	0.52	0.38
C-Band	2.13	1.82	1.33
X-Band	6.76	5.79	4.23

Fall-Spring Maritime

	300 nm	250 nm	200 nm
L-Band	0.29	0.21	0.15
S-Band	0.64	0.55	0.40
C-Band	2.26	1.91	1.37
X-Band	7.20	6.10	4.38

C. Rain Attenuation

Attenuation by moderate-to-heavy rain can be even more stressing upon microwave propagation than the attenuation by clouds. Rain attenuation is also, however, much more difficult to estimate than cloud attenuation. There are several reasons for this added complexity, among them:

- Droplet Attenuation: The Rayleigh approximation (assuming droplet size << wavelength) is not valid for theoretical predictions of scattering for the size of raindrops typically encountered (large when compared to cloud particles) and the calculations of attenuation must be based on Mie's exact formulation for spheres. This, in turn, is not precise as raindrops tend toward oblateness, while their axes of symmetry may or may not be oriented vertically, and the base of the drop may or may not be concave.[15]

- Measurement Errors: Measured rainfall attenuation tends to be appreciably higher than that predicted by theory. It has been speculated that the measured data is in error due to poor characterization of the rain field (both spectrally and temporally) during experiments and neglect of the effects of temperature and wind.[16,17] (This is discussed in detail in Appendix B.)

- Precipitation Density within Cloud: Calculated attenuations for rainfall generally deal with rainfall below cloud level and, therefore, neglect the updrafting of rain and do not deal with water content and drop size distribution within the cloud. Due to the updrafting phenomenon, radar rain attenuation within the cloud will be greater than that below the cloud. This is due to difficulties in assessing rain within clouds where updrafting of rain results in lower actual rainfall rate but higher precipitated water content.

- Drop Size Variability: Calculations and measurements of rainfall attenuation have usually not accounted for a variability in drop size distributions or in grouping of rainfall rates.[18]

- Increased Non-Precipitating Water Beneath Cloud

1. Rainfall Rate

The standard measurement for rainfall comparisons is "rainfall rate." This, however, does not accurately specify all of the significant parameters for radar attenuation, particularly for that portion of the precipitation within the cloud. For a typical cold front, the surface rain rate is about 1.2 mm/hr; for a typical warm front, the rate is about 0.6 mm/hr.[19] Within the cloud there are updrafts which will yield a much larger concentration of droplets, which can comprise a liquid water content four times greater than that in the surface rain. These drops within the cloud are, on average, assumed to be represented by a very similar drop size distribution when compared to those reaching ground. A representative plot of the rain water content, described as an effective rain rate, is shown in Figure 5.

Rain rates for a fall-spring and a winter model were pro-rated according to vertical precipitation-water concentration profiles for fall-spring and winter widespread precipitation.[2] In order to use such a pro-rating of rain rates, the conservative assumption was made that there is no dependence of drop-size distribution upon either altitude or updraft velocity. Thus rain-rate is directly proportional to precipitation-water content. Figure 5 shows the profiles pictorially.

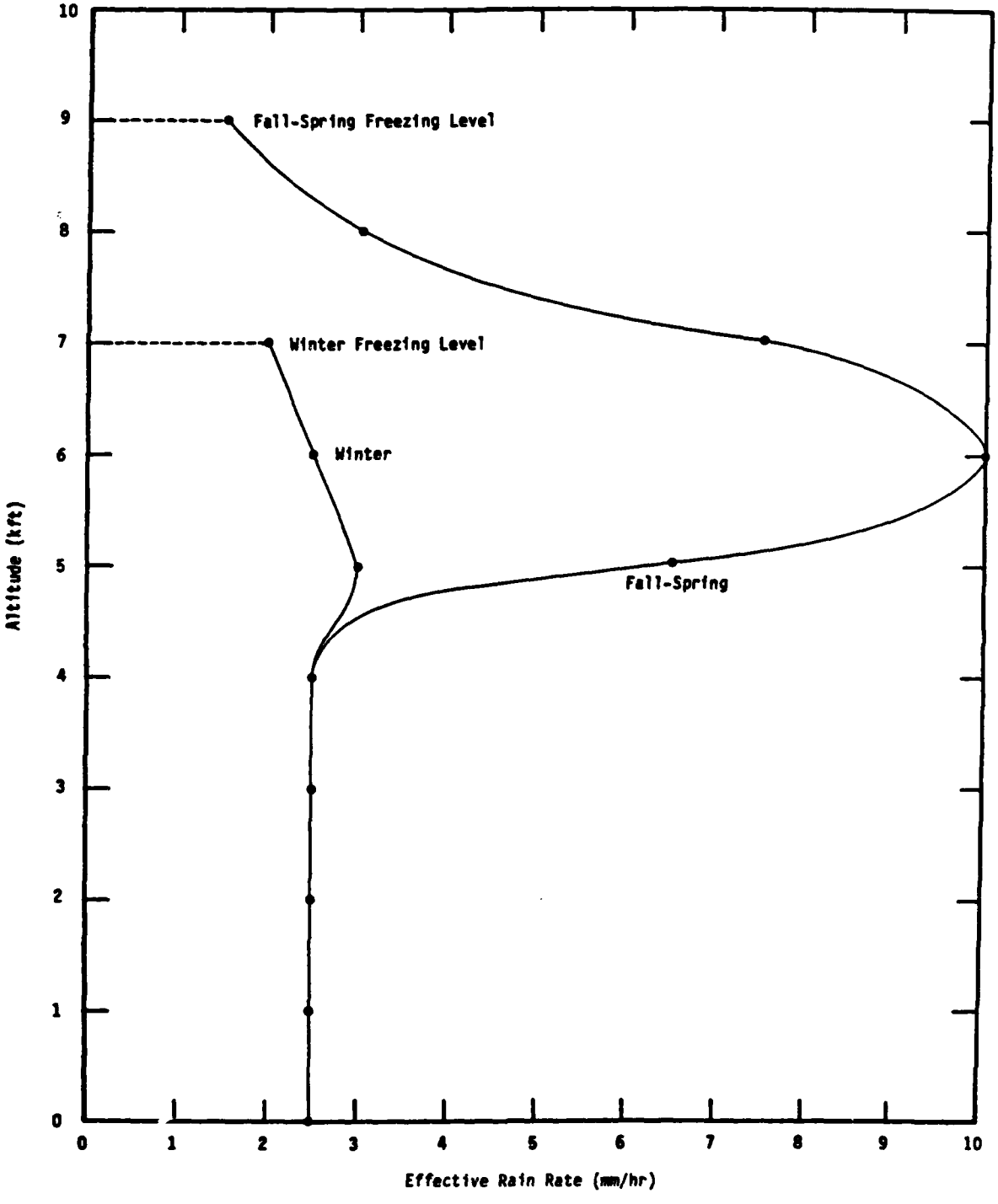

Figure 5
Effective Rain Rate versus Altitude
(due to increased water content)

2. Attenuation Calculations

For the attenuation calculations here, a light rain is assumed with 2.5 mm/hr surface rate. This would be representative of relatively strong frontal rain. While the results of theoretical calculations are widely quoted, there is only a small amount of experimental attenuation data available, and none below X-band. (The lack of experimentation at C-, S-, and L-bands occurs principally because the rain attenuation is significantly less in these bands and is extremely difficult to separate from other losses.) There is also large scatter in the X-band measurements. Table 9 compares values of the 2.5 mm/hr rain attenuation coefficient for X-band from various sources.

TABLE 9

Theoretical and Experimental Values of Rain Attenuation at X-Band
Rain Rate of 2.5 mm/hr

Source	λ (cm)	T (°C)	k (dB/km)
Theoretical Data			
Ryde and Ryde[11]	3.2	18	.0317
F. D. Dyer et al[20]	3.2	Not Given	.025
Medhurst[21]	3.0	20	.0284
Atlas et al[22]	3.2	18	.024
Hawkins and LaPlant[23]	3	Not Given	.025
Falcone et al[24]	3	20	.0311
R. M. Dyer and Falcone[25]	3.2	18	$.020 \pm .004$
Ananasso[26]	3.2	-10 to +20	.0131 to .0315
Cantor[27]	3.0	Not Given	.040
Measured Data			
Currie et al[28]	3.2	10	.055
Medhurst[29]	3.2	Not Given	$.065 \begin{matrix} + .048 \\ - .020 \end{matrix}$

There is a substantial variation between the theoretical values (using Mie theory) and experimental values of attenuation coefficient shown in Table 9. They are due primarily to:

- Poor characterization of instantaneous rain fields
- Small measurement errors produce large errors in coefficients
- Wind and temperature effects are frequently ignored
- Polarization effects are frequently not considered.

These are discussed in Appendix B.

R. M. Dyer's method[30] appears relatively thorough, including an extensive evaluation of variabilities in drop size distributions and temperature effects. This method estimates X-band attenuation to be 0.020 $\pm$ .004 dB/km for 2.5 mm/hr. Table 10 gives Dyer's figures for the normalized attenuation coefficients "k/Rain Rate" at S-, C-, and X-bands for various rain rates and temperatures.

TABLE 10

Normalized Rain Attenuation Coefficients k/R (dB km^{-1}/mm h^{-1}) and Variability From Dyer and Falcone[30]

Radar		Rain Rate	Normalized Attenuation Coefficient and Variability							
Freq. (GHz)	Wavelength (cm)	(mm h^{-1})	0°C		10° C		18° C		Averaged 0°C to 18°C	
3.0	10	3	6.9×10^{-4}	11%	4.5×10^{-4}	11%	3.0×10^{-4}	11%	4.6×10^{-4}	32%
		15	6.1×10^{-4}	5%	4.0×10^{-4}	5%	3.0×10^{-4}	5%	4.4×10^{-4}	32%
		70	6.1×10^{-4}	5%	4.0×10^{-4}	5%	3.1×10^{-4}	7%	4.4×10^{-4}	31%
5.5	5.45	3	2.9×10^{-3}	4%	2.0×10^{-3}	4%	1.5×10^{-3}	4%	2.1×10^{-3}	28%
		15	3.1×10^{-3}	17%	2.2×10^{-3}	17%	1.8×10^{-3}	15%	2.5×10^{-3}	28%
		70	4.1×10^{-3}	29%	3.3×10^{-3}	29%	2.8×10^{-3}	33%	3.4×10^{-3}	29%
9.4	3.2	3	1.1×10^{-2}	10%	9×10^{-3}	14%	8×10^{-3}	18%	9×10^{-3}	20%
		15	1.4×10^{-2}	7%	1.4×10^{-2}	11%	1.3×10^{-2}	16%	1.4×10^{-3}	11%
		70	1.7×10^{-2}	21%	1.9×10^{-2}	27%	1.9×10^{-2}	31%	1.8×10^{-2}	25%

For the radar attenuation calculations, the upper bound attenuations (the mean value plus one sigma) were used. This gives k of 0.024 dB/km at X-band (3.2 cm) for 18°C and 2.5 mm/hr rain. Since Dyer data was not calculated for L-band, the L-band attenuation was calculated by Medhurst's method.[21]

Since the data in Table 10 are not given for each of the temperatures in the layered atmosphere models used, graphs were drawn for each frequency of both the mean and standard deviation of k/R versus temperature. Figure 6 is an example for X-band. The actual values used in the attenuation calculations depended on "effective" rainfall rate, and thus deviated from a 2.5 mm/hr curve as shown by the data on Figure 6.

For actual rain, the raindrops, unlike cloud aerosols, are not in thermal equilibrium with the surrounding atmosphere, being cooler than ambient temperature. In addition, temperature gradients exist within the drops. These effects are not large, and were neglected in this analysis. The raindrops were therefore assumed to be at the ambient temperature.

Because ice attenuates much less (dB attenuation $\sim$.01 that of water droplets), the attenuation due to precipitation above the 0°C altitude was neglectable (whereas that due to supercooled cloud droplets was not). Also the increased attenuation in the few hundred feet of the "bright band" just below the freezing altitude was treated as if it were the attenuation due to totally liquid droplets instead of the larger partially melted ice particles with liquid exteriors common to the "bright band."

Table 11 is an example of fall-spring X-band rain attenuation calculations. Attenuation coefficients and sigmas (σ) were figured from Figure 6, and multiplied by the layer path length (Δ). These were then summed over all layers and doubled to yield a final two-way rain attenuation. Table 12 gives results for both seasons in each radar band.

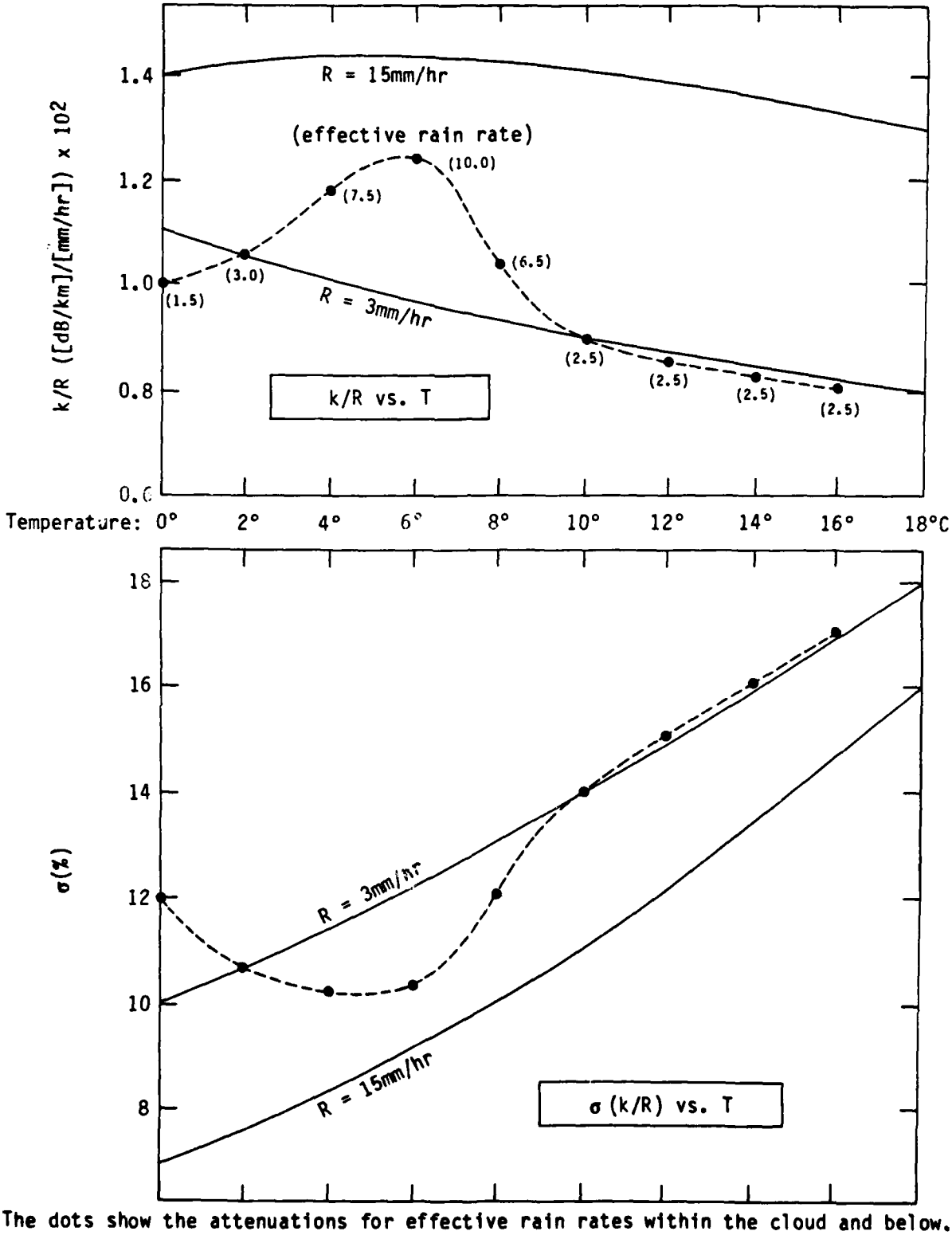

Figure 6. Fall-Spring k/Rain Rate and σ vs. Temperature for λ = 3.2 cm

TABLE 11

X-Band Rain Attenuation
for Fall-Spring Maritime Model

h(ft)	T (°C)	Effective R(h) mm/hr	$\bar{k}(h,T)$ dB/nm	$1+\sigma$	k(h,T) dB/nm	Δ nm	A_R dB
200							
	16	2.5	.0380	1.17	.0444	24.38	1.0830
1,000							
	14	2.5	.0389	1.16	.0451	16.67	0.7521
2,000							
	12	2.5	.0403	1.15	.0463	12.63	0.5851
3,000							
	10	2.5	.0417	1.14	.0475	10.52	0.4997
4,000							
	8	6.5	.1300	1.12	.1456	9.24	1.3455
5,000							
	6	10.0	.2296	1.10	.2526	8.12	2.0512
6,000							
	4	7.5	.1625	1.10	.1788	7.66	1.3693
7,000							
	2	3.0	.0583	1.11	.0648	7.16	0.4636
8,000							
	0	1.5	.0278	1.12	.0311	6.68	0.2078
9,000							8.3573
						2-way	16.71 dB

TABLE 12

Rain Attenuation for L-X Bands

Radar Band - Wavelength \ Model	Fall-Spring Maritime	Winter Maritime
L - 16 cm	0.22 dB	0.17 dB
S - 10 cm	0.74	0.55
C - 5.4 cm	3.38	2.20
X - 3.0 cm	16.71	9.43

Rain was also examined for the effects of reduced radar elevation angle, as was done for the cloud case. Table 13 shows representative calculations for fall-spring rain attenuation in the 200 and 250 nm paths for X-band. Table 14 gives the results for both seasons and each radar band.

D. Total Attenuation

Table 15 gives the cloud, rain, and total weather attenuations for the seasons, ranges, and radar bands discussed above. Table 16 combines these results with the atmospheric attenuation over a 300 nm path.

TABLE 13

X-Band Rain Attenuation at Reduced Ranges

Fall-Spring Maritime Model

h (feet)	200 nm			250 nm		
	k(h,T) dB/nm	Δ nm	A_{cloud} dB	k(h,T) dB/nm	Δ nm	A_{cloud} dB
200						
	.0444	4.15	.1843	.0444	8.16	.3623
1,000						
	.0451	5.00	.2255	.0451	9.08	.4095
2,000						
	.0463	4.87	.2255	.0463	8.27	.3829
3,000						
	.0475	4.70	.2233	.0475	7.57	.3596
4,000						
	.1456	4.56	.6639	.1456	7.05	1.0265
5,000						
	.2526	4.47	1.1291	.2526	6.66	1.6823
6,000						
	.1788	4.31	.7706	.1788	6.27	1.1211
7,000						
	.0648	4.25	.2754	.0648	6.00	.3888
8,000						
	.0311	4.13	.1284	.0311	5.70	.1773
9,000						
			3.8260			5.9102
			2-Way = 7.65 dB			2-Way = 11.82 dB

TABLE 14

2-Way Rain Attenuation for 200-300 nm Ranges

Fall-Spring Maritime

	Range		
	300 nm	250 nm	200 nm
L-Band	0.22 dB	0.15 dB	0.36 dB
S-Band	0.74	0.53	1.08
C-Band	3.38	2.43	4.34
X-Band	16.71	11.82	17.92

Winter Maritime

	Range		
	300 nm	250 nm	200 nm
L-Band	0.17 dB	0.10 dB	0.06 dB
S-Band	0.55	0.33	0.20
C-Band	2.20	1.34	0.81
X-Band	9.43	5.65	3.42

TABLE 15

Cloud, Rain, and Total Weather Attenuation

Range	Frequency	Fall-Spring Maritime			Winter Maritime		
		Clouds	Rain	Total	Clouds	Rain	Total
300 nm							
	L-Band	0.29	0.22	0.51	0.24	0.17	0.41
	S-Band	0.64	0.74	1.38	0.61	0.55	1.16
	C-Band	2.26	3.38	5.64	2.12	2.20	4.32
	X-Band	7.20	16.71	23.91	6.76	9.43	16.19
250 nm							
	L-Band	0.21	0.15	0.36	0.21	0.10	0.31
	S-Band	0.55	0.53	1.08	0.52	0.33	0.85
	C-Band	1.91	2.43	4.34	1.82	1.34	3.16
	X-Band	6.10	11.82	17.92	5.79	5.65	11.44
200 nm							
	L-Band	0.15	0.10	0.25	0.15	0.06	0.21
	S-Band	0.40	0.35	0.75	0.38	0.20	0.58
	C-Band	1.37	1.58	2.95	1.33	0.81	2.14
	X-Band	4.38	7.65	12.03	4.23	3.42	7.65

TABLE 16

Total Path Propagation Attenuation for 300 nm Range

Frequency Band	Fall-Spring Maritime				Winter Maritime			
	Atmosphere	Clouds	Rain	Total	Atmosphere	Clouds	Rain	Total
L-Band	3.3	0.3	0.2	3.8 dB	3.3	0.2	0.2	3.7 dB
S-Band	3.6	0.6	0.7	4.9 dB	3.6	0.6	0.6	4.8 dB
C-Band	4.5	2.3	3.4	10.2 dB	4.5	2.1	2.2	8.8 dB
X-Band	5.5	7.2	16.7	29.4 dB	5.5	6.8	9.4	21.7 dB

E. Thunderstorms

Thundershowers have severe local radar attenuation, but are relatively small in breadth and occur a small percentage of the total time. The worldwide occurrence of thunderstorms is given in Charts 1-4 for each of the seasons after U.S. Naval Weather Service Data.[31] This data clearly shows that the occurrence of thunderstorms in most areas of operational significance to the U.S. Navy is relatively limited, with the largest incidence being over tropical land areas.

A study of thunderstorms in central New England[32] was conducted by P.M. Austin at MIT's Lincoln Laboratory in the 1960s. Data from this study indicated that for a ground radar looking at elevation angles above 5° (the reciprocal of an airborne radar looking down at -5°) severe attenuation (10 dB or more at 10 GHz) would be encountered less than 6 hours per year along each particular azimuth and less than 30 hours per year in any direction. Figure 7, showing Austin's results extrapolated to the horizontal, indicates that at 0° elevation the severe attenuation would be encountered less than 10 hours per year at a single azimuth and less than 80 hours per year in any direction. If the airborne radar is conducting surveillance over no more than 180°, a figure of about 40 hours per year is typical and amounts to less than 0.5% of a year. Data in Charts 1-4 extends the Austin data beyond New England and confirms this figure (0.5%) as an upper bound on the occurrence of severe radar attenuation due to thunderstorms in Navy operational areas.

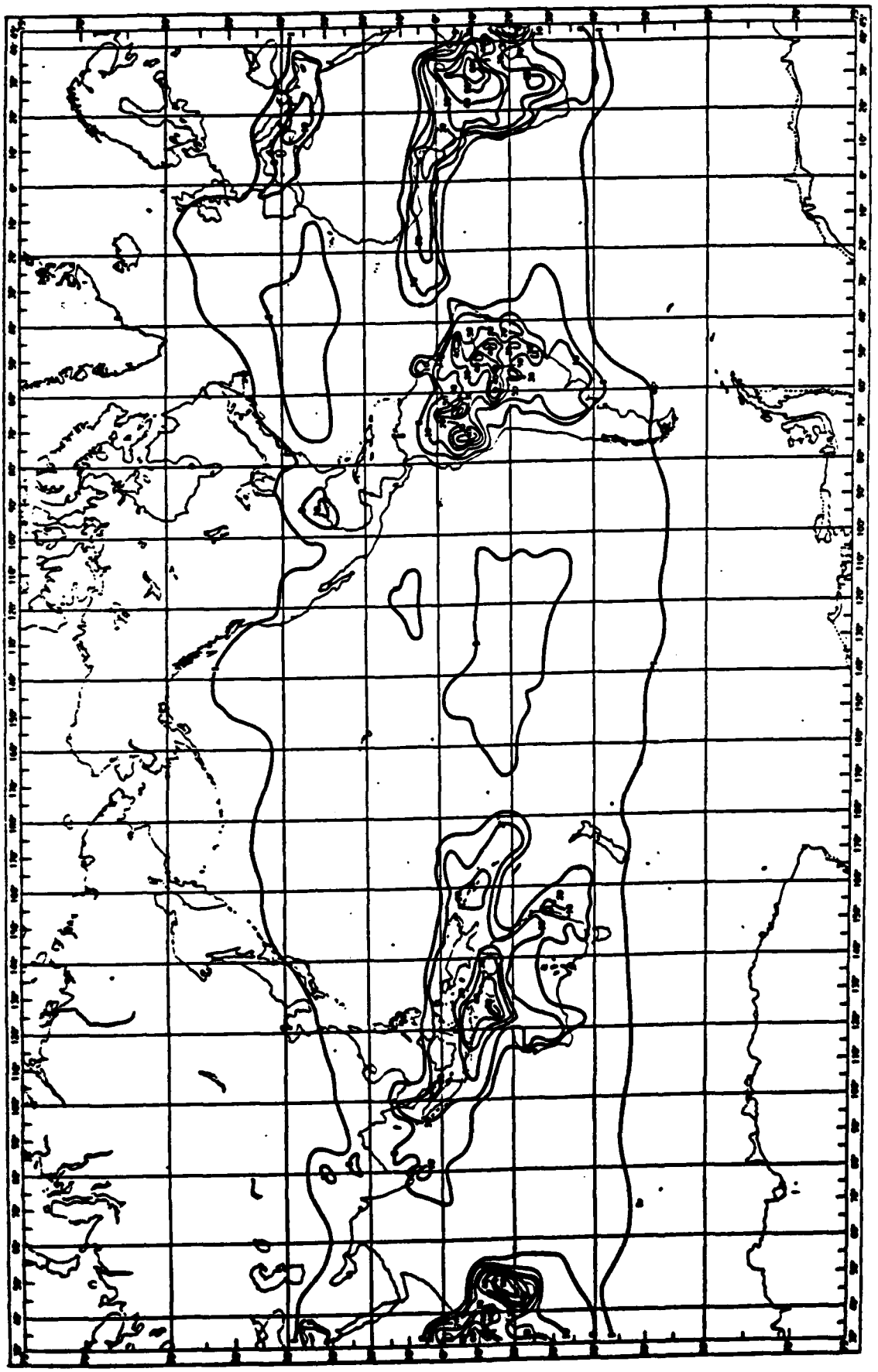

Chart 1. DEC - JAN - FEB Average number of days with THUNDERSTORMS

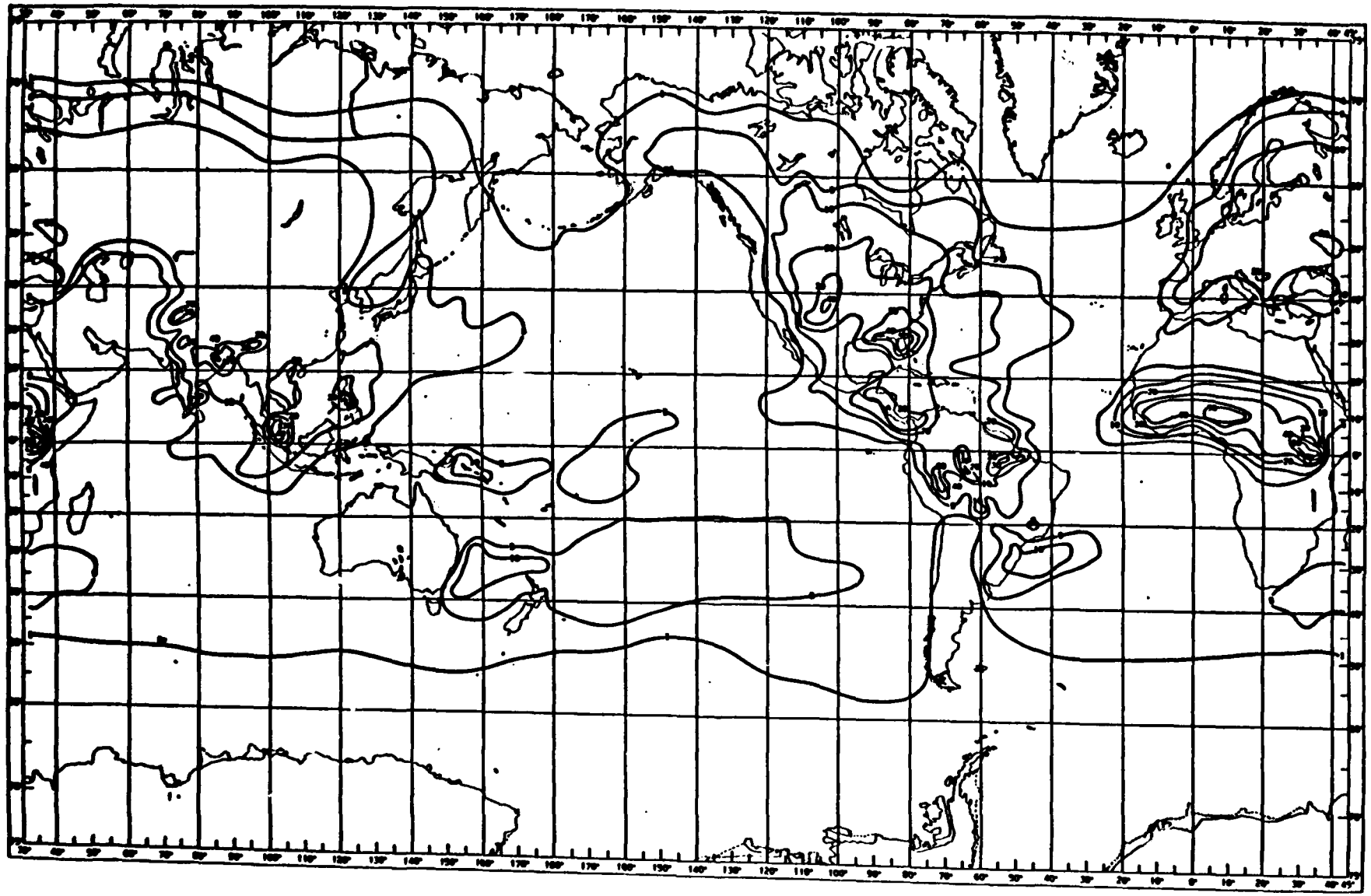

Chart 3. JUN - JUL - AUG Average number of days with THUNDERSTORMS

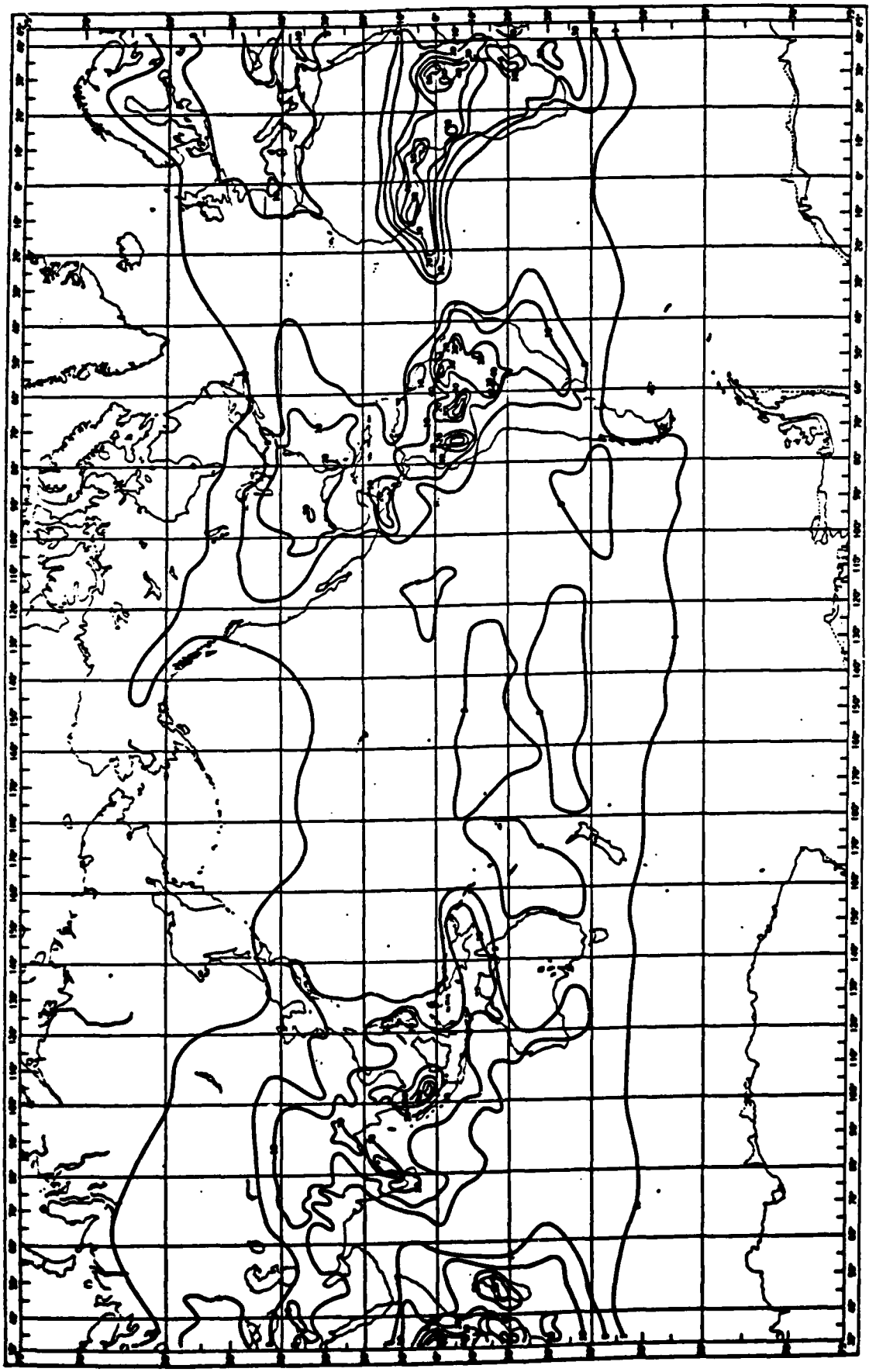

Chart 2. MAR - APR - MAY Average number of days with THUNDERSTORMS

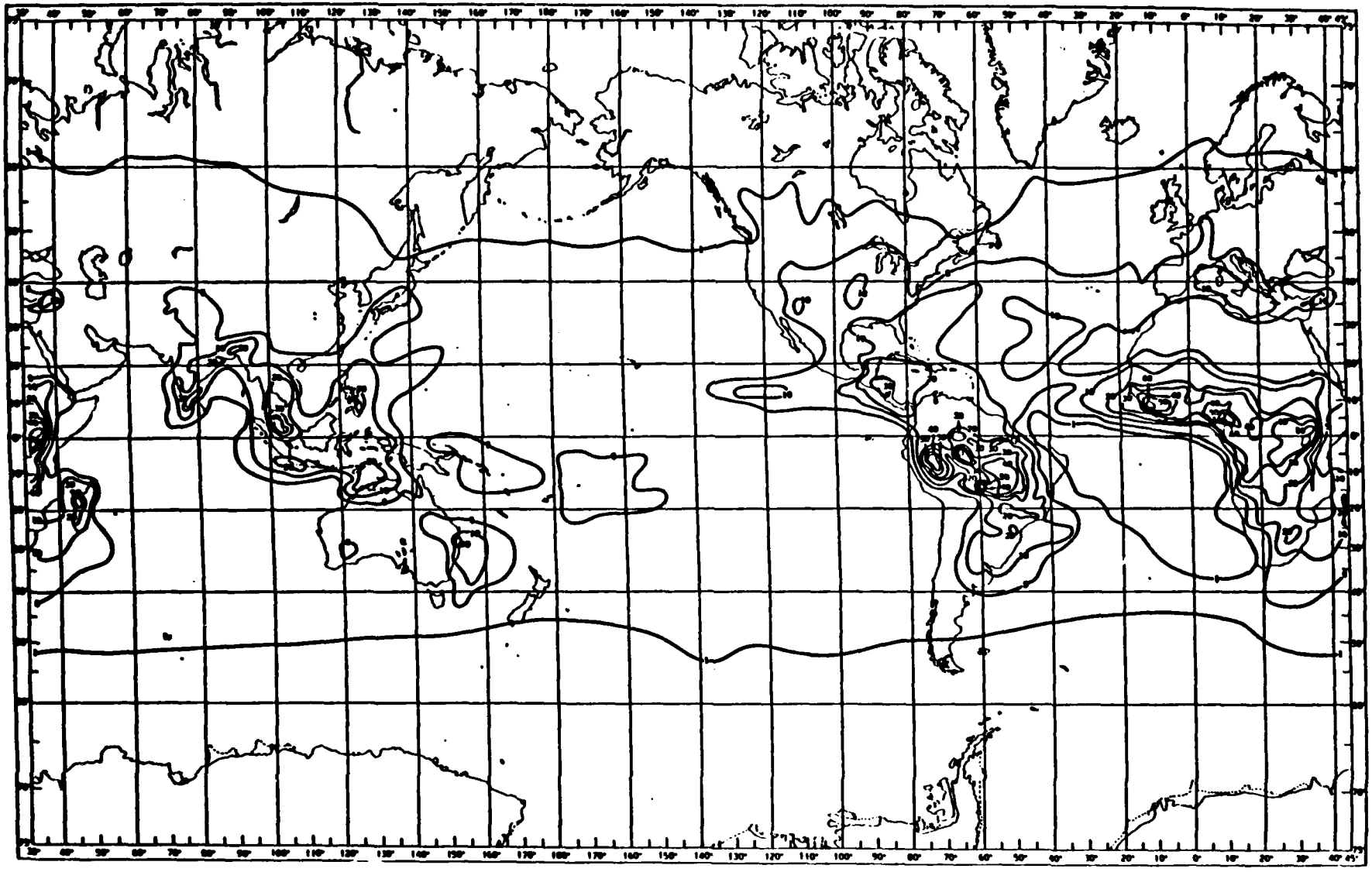

Chart 4. SEP - OCT - NOV Average number of days with THUNDERSTORMS

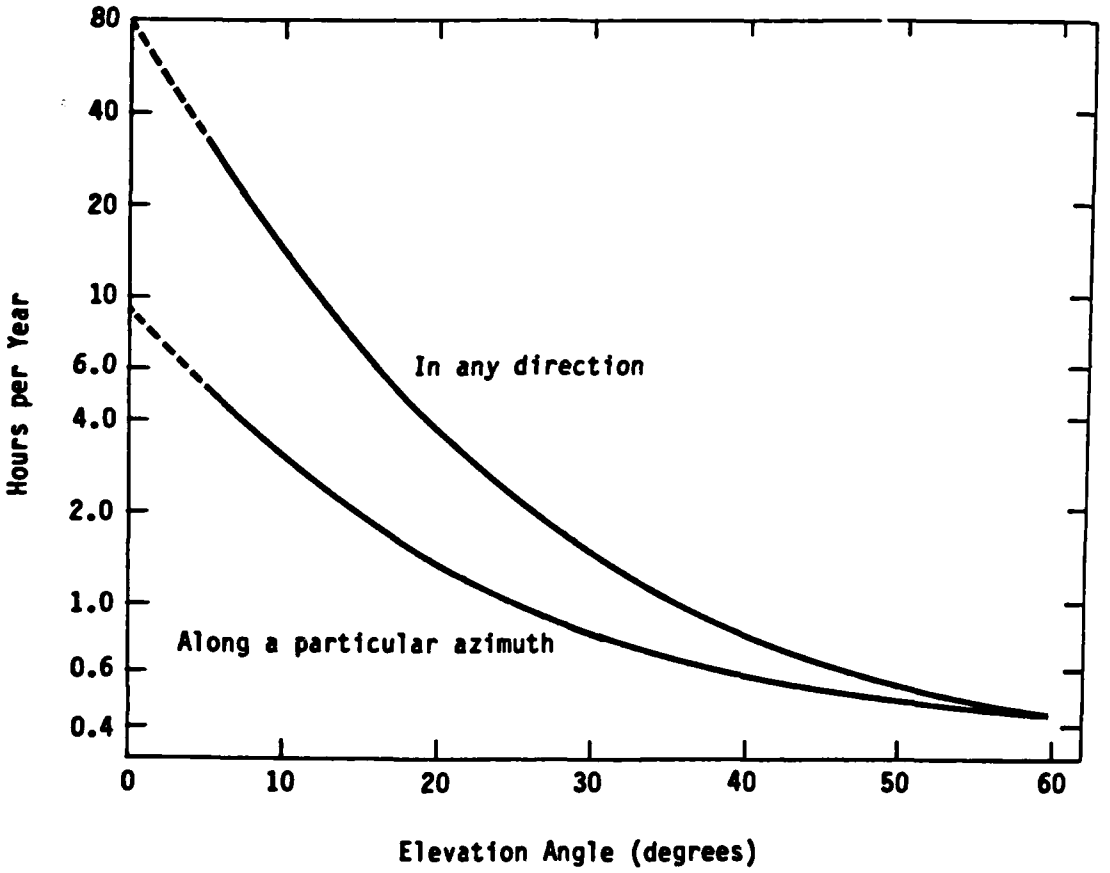

Figure 7. Thunderstorm Occurrence in Central New England

Number of hours per year of severe attenuation (10 db or more of 10 GHz radiation) by intense thunderstorms for stations in central New England.

REFERENCES

1. Prupacher, Hans R. and Klett, James D.; The Microphysics of Clouds and Precipitation; D. Reidel; Boston; 1978; pp. 18-19.

2. Atlas, David; "Model Atmospheres for Precipitation;" Section 5.? of the Handbook of Geophysics and Space Environments; Shea L. Valley, Ed.; McGraw-Hill; New York; 1965.

3. James, W.; The Effect of Weather in Eastern England on the Performance of X-Band Ground Radars; RRE Technical Note 655; Malvern, Worcs., U.K.; 1961.

4. Atlas, David (Ref. 2), p. 5-9.

5. Mason, B. J.: The Physics of Clouds; Clarendon Press; Oxford; 1971.

6. Gossard, Earl E. and Strauch, Richard G.; Radar Applications in Cloud and Clear-Air Studies; Wave Propagation Laboratory, WPL-87; Boulder, Colorado; 1981.

7. Davidson, K.; Personal Communication; 1 Feb. 1982; Meteorology Dept.; Monterey, CA.

8. Bean, B. R., Dutton, E. J., and Warner, B. D.; "Weather Effects on Radar," Chapter 24 of Radar Handbook; M. Skolnik, Ed.; McGraw-Hill; New York; 1970, p. 24-22.

9. Donaldson, R. J., Jr., "The Measurement of Cloud Liquid-Water Content by Radar," J. Meteorol., Vol. 10, June 1953, p. 204-221.

10. Mason (Ref. 5), p. 291.

11. Ryde, J. W. and Ryde, D.; "Attenuation of Centimetre and Millimetre Waves by Rain, Hail, Fog, and Clouds;" GEC Report 8670, May 1945.

12. Gunn, K.L.S. and East, T.W.R.; "The Microwave Properties of Precipitation Particles;" Quart. J. Roy. Meteorol. Soc.; Vol. 80, Oct.-Dec. 1954; pp. 522-545.

13. Chen, C. C.; Attenuation of Electromagnetic Radiation by Haze, Fog, Clouds, and Rain; Rand Corporation; Santa Monica, California; R-1694-PR; 1975; p. 11.

14. Van Vleck, J. H., Purcell, E. M., and Goldstein, Herbert; "Atmospheric Attenuation;" Chapter 8 of Propagation of Short Radio Waves; Donald E. Kerr., Ed.; McGraw-Hill; 1951; New York.

15. Gossard, Earl E. and Strauch, Richard G.; Radar Applications in Cloud and Clear-Air Studies; NOAA Tech. Memo ERL WPL-87; 1981; p. 128-144.

16. Medhurst; Richard G.; "Rainfall Attenuation of Centimeter Waves: Comparison of Theory and Measurement;" IEEE Trans. on Antennas and Propagation; AP-13:557; 1965.

17. Falcone, V. J., Jr., and Dyer, R.; "Refraction, Attenuation, and Backscattering of Electromagnetic Waves in the Troposphere: A Revision of Chapter 9, Handbook of Geophysics and Space Environments;" AFCRL-70-0007; 1970; p. 26.

18. Dyer, R. M. and Falcone, V. J.; "Variability in Rainfall Rate Attenuation Relations;" AFCRL; Bedford, Mass.; Undated; p. 1.

19. James, W. (Ref. 3), p. 4.

20. Dyer, F. D., et al; "Radar Backscatter from Land, Sea, Rain, and Snow at Millimeter Wavelengths;" Eng. Exp. Station; Georgia Inst. of Technology, Atlanta, Georgia; 1977.

21. Medhurst (Ref 16); p. 556.

22. Atlas, David, et al; "Some Aspects of Electromagnetic Wave Propagation;" Chapter 9 of Handbook of Geophysics and Space Environments; Shea L. Valley, Ed.; McGraw-Hill; New York; 1965.

23. Hawkins, H. E. and LaPlant, O.; "Radar Performance Degradation in Fog and Rain;" IRE Trans. on Aeronautical and Navigational Electronics; March 1959:28.

24. Falcone, V. J., Jr., et al; "Atmospheric Attenuation of Millimeter and Submillimeter Waves: Models and Computer Code;" AFGL-TR-79-0253; 1979.

25. Falcone, V. J., Jr., and Dyer, R. (Ref. 17); p. 2.

26. Ananasso, Fulvio; "Coping with Rain Above 11 GHz;" Microwave System News; March 1980.

27. Cantor, Israel; "Rainfall Effects on Satellite Communications in the K, X, and C Bands;" U.S. Army ECOM-5459; 1972; AD 751 742.

28. Currie, N. C., et al; "Some Properties of Radar Returns from Rain at 9.375, 35, 70, and 95 GHz;" Georgia Inst. of Technology; IEEE Intl. Conf.; 1975.

29. Medhurst (Ref. 16); p. 559.

30. Dyer, R. and Falcone (Ref. 18); p. 3.

31. U.S. Naval Weather Service Command; Study of Worldwide Occurrence of Fog, Thunderstorms, Supercooled Low Clouds, and Freezing Temperatures; NAVAIR 50-1C-60; December 1971.

32. Austin, Pauline M.; Frequency of Occurrence of Rain Attenuation of 10 dB or Greater at 10 GC; Massachusetts Institute of Technology, Lincoln Laboratory; December 1966.

33. Breed, D. W., Grant, L. O., Dye, J.; "Cloud Droplet Distribution in High Elevation Continental Cumulus;" Proc. Intern. Conf. on Cloud Physics; Boulder, Colorado; 658-664; 1976.

APPENDIX A

CLOUD DENSITIES

To calculate anticipated attenuation in clouds, the cloud liquid water content must be known. This figure, however, may not be known with much precision. Some radar texts quote densities of typical clouds without identifying types of cloud. The Radar Handbook, by Skolnik[8] (p. 24-22), for instance, quotes Donaldson in giving observational values of cloud densities over the range of 1 to 2.5 gm/m^3. The Donaldson data were acquired by radar prior to 1956. During the 1950s and 1960s, however, radar was not a good tool for the observation of clouds. It has only been during the 1970s with the utilization of dual frequencies, dual polarization, and doppler processing that radar has been capable of making quality cloud observations (see Gossard[15] - p. 116). Therefore, in-situ measurements should be considered for cloud parameters.

Various methods have been used to make in-situ measurements, mostly from powered or glider aircraft. The methods include:

- photography
- exposing to the airstream slides coated with grease or some other material which retains either the droplets or their impressions for later sizing and counting, and
- various active and passive optical scattering measurement devices.

Some of these results along with the Radar Handbook data are summarized in Table A-1.

As can be seen in the table, the values quoted in Skolnik seem to be high for clouds in general. Even small cumulus clouds may have low water content due to mixing with outside air. The experimental techniques have differed, but

it seems fair to state that the values used in the body of this paper for densities are appropriate and lead to values of cloud attenuation that are about one-sixth what they would have been had the value of 2.5 gm/cm^3 quoted in Skolnik been used.

TABLE A-1

CLOUD MOISTURE CONTENT MEASUREMENTS

Reference	Year Reported	Cloud Type	Water Content (gm/m^3)
1. Bean et al,[8] in Radar Handbook:			
• Weickmann and Aufm Kampe	1953	Cumulus congestus	4.0
• Donaldson, R. J., Jr.[9]	1955	---	1-2.5
2. Mason[5] and Gossard[15]			
• Weickmann and Aufm Kampe	1953	Fair weather cumulus Cumulonimbus Cumulus congestus	1.0 2.5 3.9
• Squires	1958	Continental cumulus Tradewind cumulus Hawaiian dark stratus	0.35 0.81 0.335
• Kazas		Hawaiian orographic Altostratus	0.523 0.6
• Diem	1948	Fair weather cumulus Cumulus congestus Stratocumulus Altostratus Nimbostratus Stratus	0.32 0.87 0.09 0.28 0.40 0.29
3. Mason[5]			
• Warner and Newnhan	1952	Stratocumulus	0.3
• Kline and Walker	1951	Stratocumulus	0.06 to 1.30 (avg = 0.30)
• Neiburger	1949	Stratus (1600 ft thick)	0.67 (max.)
4. Breed et al[33]	1976	Cumulus	0.015 to 0.405

APPENDIX B

RAINFALL ATTENUATION - THEORY AND EXPERIMENT

There are several problems related to the measurement of rainfall attenuation which seriously degrade the accuracy of the results and force greater reliance on theoretical calculations for predicting attenuation; they include:

- Poor characterization of the rain field
- Non-typical raindrop size distributions
- Large attenuation coefficient errors produced from small measurement errors
- Wind effects neglected
- Temperature effects frequently neglected
- Polarization effects frequently neglected.

The first problem that confronts the experimentalist in measuring rainfall attenuation is measuring the rainfall. There is an inherent conflict at the lower frequencies which is difficult to resolve: if the antenna spacing in an experiment is small, attenuation will be too small to measure; and as path length is increased the likelihood of a uniform precipitation field is decreased.

In the single X-band experiment cited by Medhurst, only a single rain gauge was used; in one of two cases it was displaced from the line of sight by 1000 ft and at the transmitter end of the antenna line of sight, and in the other case, it was 500 ft offset from the antenna line of sight and at the receiver end. The path length was 900 feet. Additionally, the rain gauges gave only average rain rates over approximately one-minute intervals. Other sources have apparently found that this (60 sec) is about the greatest length of time for temporal uniformity of rain, and the odds are therefore against these rain rates being uniform in time over the period of collection.

The Medhurst data were collected during two storms, one of which had rainfall rates up to 130 mm/hr. The environmental conditions in these storms would probably vary substantially from that typical of frontal rain even for similar rain rates.

Another problem is that small errors in measurements of signal losses, when the signal losses were small to begin with, could lead to large relative errors and hence large errors in the attenuation coefficients. The data cited by Medhurst suggests a mean value of 0.12 dB/nm in a band between 0.22 and 0.07 dB/nm (0.12 dB/nm + 84% or - 42%), demonstrating considerable scatter. Reducing the relative size of the errors by increasing the attenuation, which could be accomplished by lengthening the path, would worsen the characterization of the rain field.

Neglect of wind effects is another potential error source or problem. There is evidence to show that winds in general, and gusting winds in particular, will reduce rain drop velocity and thus support larger amounts of water than calm air given the same surface rainfall rate, hence increasing the total amount of water present in the air and therefore attenuation. Rain rate can be described by:

Rain Rate = (Volume of water/Volume) x (Velocity of water drops)

Thus it can be seen that wind updrafts that decrease drop velocity will greatly affect water volume and rain rate.

An additional error source is neglect of temperature effects. Figure B-1 shows the temperature correction factors of interest to this paper. The factors make allowance for the temperature dependence of the complex index of refraction of water. The range of values for X-band at 2.5 mm/hr is about 20%, or 0.82 to 1.03. Temperatures are not given for the X-band measurements in Medhurst.

Still another error source arises from polarization effects on drops which have departed from spherical shape. Since such departures are nearly always toward the prolate, horizontally polarized waves are attenuated more than vertically polarized. For X-band and 2.5 mm/hr, an increase of 2.5% would occur over the perfect spherical case.

The possible summing of all these effects can yield large differences between different measurements and between measured and calculated values.

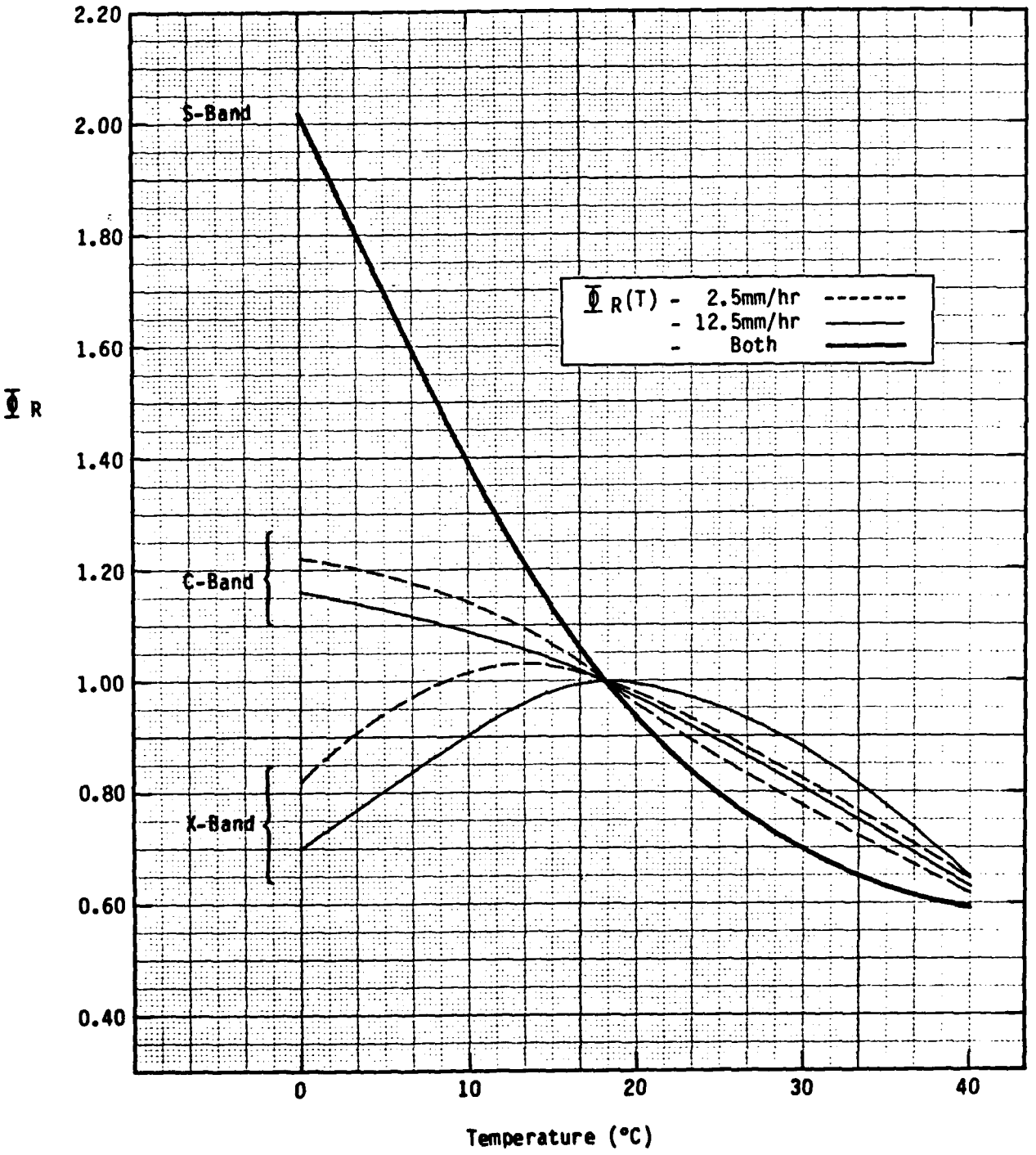

Figure B-1

Temperature Correction Factors for Complex Index of Refraction in Rain